Pertanika J. Sci. & Technol. 28 (3): 1105 - 1116 (2020)

PERTANIKA JOURNALS

SCIENCE & TECHNOLOGY

Journal homepage: http://www.pertanika.upm.edu.my/

Impact of Lateral Size of Graphene Oxide in Pour Point Depressant Composite on Wax Crystallisation of Model Oil

Muhamad Ridhwan Hafiz Rosdi, Mohd Danial Mohd Johary, Ku Marsilla Ku Ishak and Azlan Ariffin*

School of Materials and Mineral Resources Engineering, Engineering Campus, Universiti Sains Malaysia, 14300 USM, Nibong Tebal, Penang, Malaysia

ABSTRACT

Graphene oxide (GO) is a reliable additive used to improve the wax crystal inhibition performance of pour point depressant (PPD). In understanding the lateral size effect on wax crystal inhibition, PPD emulsions containing graphene oxide of different lateral sizes were prepared. The parameters of pour point reduction (PPR) and dissipated wax crystallisation enthalpy were considered in the assessment of wax inhibition performance. PPR was measured using a pour point tester in accordance to ASTM D-97, while the enthalpy dissipation was evaluated via differential scanning calorimetry (DSC) under cooling cycle. The study revealed that the addition of GO lowered the wax crystallisation enthalpy, as indicated by the lesser amount of precipitated wax present in the model oil. The enthalpy underwent a decrease from 25.04 to 23.97 Jg^{-1} with decreasing GO lateral size. It is evident from the pour point test that the use of different GO lateral sizes significantly affects the wax inhibition, as verified through the highest PPR of 10°C displayed by the EJGO5 sample (with addition of the smallest lateral size of 1 µm). In short, manipulating the GO lateral size in sonicated samples boosted the PPR up to 100% compared to the unsonicated sample (EJGO1). Furthermore, smaller lateral size provides more nucleation site for wax co-crystallisation, hence preventing the neighbouring wax crystals from attaching and forming a looser crystal structure. The thermal characteristics of the PPD

ARTICLE INFO

Article history:
Received: 26 February 2020
Accepted: 22 April 2020
Published: 16 July 2020

E-mail addresses:
piecedue@yahoo.com (Muhamad Ridhwan Hafiz Rosdi)
duerensuke@gmail.com (Mohd Danial Mohd Johary)
ku_marsilla@usm.my (Ku Marsilla Ku Ishak)
srazlan@usm.my (Azlan Ariffin)
*Corresponding author

ISSN: 0128-7680
e-ISSN: 2231-8526

emulsions were also examined through DSC technique, which revealed that the emulsions thermal properties were unaffected by the addition of GO.

Keywords: Ethylene vinyl acetate, graphene oxide, lateral size, pour point depressant, wax crystallisation

INTRODUCTION

The precipitation of paraffin wax presents significant impacts on the waxy crude oil transportation. Paraffin wax tends to precipitate from oil due to super-saturation which takes place when the temperature of waxy crude oil falls below its wax appearance temperature (WAT) (Deshmukh & Bharambe, 2008; Martínez-Palou et al., 2011; Pedersen & Rønningsen, 2003; Yang et al., 2015). In this instance, chemical treatment such as pour point depressant (PPD) is preferred to hinder the deposition of wax, since chemical treatment is more cost-effective and efficient compared to other techniques. In general, most conventional PPD products formulated in solution are susceptible to solidification at low temperatures. Therefore, the application of PPD solution in cold climates such as the winter season is limited. To solve the PPD solidification issue at room temperature, emulsion technology is often implemented (Razak et al., 2018; Rosdi et al., 2016; Umoruddin et al., 2019).

Admiral et al. (2016) had successfully formulated flowable PPD emulsion at ambient temperature with enhanced viscosity at room temperature, thermal properties at sub ambient temperature, particle size, and stability. However, even though PPD emulsion demonstrates decent thermal and stability performances, the wax inhibition performance remains limited. Recently, graphene and graphene oxide (GO) have attracted the interest and attention of researchers as additives for wax inhibition enhancement. Indeed, the introduction of nano-sized particles into polymers has also been recognised as a well-acknowledged technique for boosting the present polymers properties (Boccaccini et al., 2010; Kim et al., 2017; Zhao et al., 2018). This specific polymer classification, known as polymer nanocomposites, can be utilised in PPD emulsion to increase its performance effectiveness. The addition of GO provides more nucleation site in emulsion, hence preventing the formation of a massive 3-dimensional crystal network structure while simultaneously enhances the flow ability of the emulsion. Al-Sabagh et al. (2016) pointed out that the addition of GO into conventional polymethylmethaacrylate (PMMA) results in superior performance by lowering the apparent viscosity and pour point of crude oil. Similarly, Sharma et al. (2019) demonstrated that significant depression in pour point could be improved with an incorporation of higher percentage GO in PPD-GO additives.

To date, most studies are focussing on the application of GO with particular dosage or concentration as well as its lateral size effects restrictedly towards the mechanical, electrical, and thermal conductivity properties of PPD material (Kim et al., 2017; Li et

al., 2019). Nonetheless, the influence of lateral size of GO on the wax crystallisation of model oil still remains unclear to be discussed. Therefore, in this study, an experiment was constructed to examine the effect of GO lateral size (with different sonication times) on the wax crystallisation behaviour and the wax crystal microstructure of model oil. Moreover, the lateral size impacts on the PPD emulsions thermal properties and stability were also examined to ensure their standard properties were not compromised.

MATERIALS AND METHODS

Materials

The tall oil fatty acid based emulsifier (MWV01), hydrocarbon solvent (Solvesso 150), and xylene utilised in this study were provided by ACME Chemicals (Malaysia) Sdn. Bhd. Meanwhile, the ethylene glycol, ethylene vinyl acetate (EVA, 25% VA content), and diethanolamine were procured from Merck Sdn. Bhd., and the graphene oxide was supplied by Nano Malaysia Berhad. Deionised water on the other hand was directly available in the laboratory.

Graphene Oxide Preparation

Sonication process was chosen in the preparation of the different lateral sizes GO. GO was weighed (0.3 gram) and dispersed in deionised water in a 50 ml glass beaker, producing GO of concentration of 10 mg/L. The beaker was then placed in ice bath to contain the heat generated from the sonication. The sonication amplitude was set to 25%. The designated GO samples as control/unsonicated (GO1) and sonicated (GO2-5) were subjected to respective sonication times, as presented in Table 1.

Table 1
Graphene oxide (GO) sample preparation based on sonication duration parameter

	GO1	GO2	GO3	GO4	GO5
Sonication duration (minutes)	0	10	30	60	100

Sample Preparation

The preparation of nano-hybrid PPD was undertaken by blending together EVA, Solvesso 150, xylene, diethanolamine, MWV01 emulsifier, ethylene glycol, and deionised water at a stirring speed of 600 rpm for 60 minutes at 50 - 60°C. Subsequently, the GO1 sample was added into the mixture accordingly and the mixture was sonicated for 10 minutes. Ice bath was used to ensure the mixture temperature not exceeding 60°C. This emulsion was denoted as EJGO1. As for the EJN sample, no addition of GO was involved. The same procedure was repeated using GO2 - GO5 samples to produce EJGO2 - EJGO5 emulsions accordingly.

Sample Characterisation

Scanning Electron Microscopy (SEM). To prepare the testing sample, a drop of sonicated GO was initially deposited on a silicon wafer (1 x 1 cm) and was left to dry in an oven for approximately 30 min. The silicon wafer, once completely dried, was attached to the sample holder using double-sided copper tape. The sample was then coated with gold to ensure it was in conductive state prior to SEM analysis. The lateral sizes of the GO1, GO2, GO3, GO4, and GO5 samples were measured through the Image J software.

Thermal Properties of PPD Composite Emulsion. The PPD composite thermal properties were assessed using Mettler Toledo (USA) differential scanning calorimeter (DSC) at a low temperature range. The samples were weighed to approximately 8 - 10 mg, then analysed at temperatures between 50°C and -30°C at a cooling/heating rate of 10°C/minute. In the first cycle, the samples were heated from 30°C to 50°C and held at an isothermal temperature of 50°C for 1 min before cooling to -30°C under the same condition as mentioned above.

Performance Evaluation via Pour Point (ASTM D-97). The evaluation was carried out according to the pour point standard of ASTM D97. This standard is generally applied to measure the pour point of any petroleum-based oil. In this evaluation, model oil sample was transferred into a glass tube and was pre-heated up to 50°C, followed by a cooling process to enable the formation of paraffin wax crystals within the model oil. When the sample temperature started to drop, its flow features were observed at every 1°C interval. The glass test tube was then tilted to spot for any model oil movement. Once no more model oil flow was observed (in tilting position), the tube was placed horizontally for approximately 10 seconds. If the test sample did not display any flow behaviour, the pour point was recorded. The pour point reduction (PPR) was then determined based on Equation 1.

$$P_R = P_B - P_{PPD} \quad (1)$$

P_R = Pour point reduction.
P_B = Pour point of untreated model oil.
P_{PPD} = Pour point of treated model oil.

Thermal Analysis of Treated Wax. Differential scanning calorimetry (DSC) has been comprehensively employed in the wax appearance temperature (WAT) investigation. Herein, the untreated/treated samples (8 - 10 mg) were analysed at temperatures between 30°C and -100°C (5°C/min). The samples were cooled from 30°C to -100°C and held at -100°C (isothermal temperature) for 1 min before undergoing heating from -100°C to 30°C at a rate of 5°C/min.

Polarised Optical Microscopy (POM). The microstructure of the untreated/treated waxes in model oil was inspected using BX51 (Olympus Optical Co., Ltd., Japan) polarising

optical microscope. The simulated paraffin wax was heated to 50°C in water bath. Subsequently, approximately 4 µL of the paraffin wax was dropped onto a round glass slide before sandwiching it together with another slide. The round glass slide was then placed on the heating stage and heated to 50°C at a rate of 5°C/min in oxygen environment. The microstructure of the waxes was recorded during the cooling process (1ºC/min) under 100X magnification.

RESULTS AND DISCUSSION

Graphene Oxide Lateral Size Analysis

Scanning electron microscopy (SEM) was conducted to measure the GO lateral size respective of different ultrasonication times. The GO samples were designated as control/ unsonicated (GO1) and sonicated (GO2 - GO5). Figure 1 (A - E) displays the SEM images of all GO samples (GO1 - GO5) at 300X magnification.

Figure 2 on the other hand exhibits the relationship between sonication time and the lateral size of the GO samples. Clearly, a considerable decrement in the GO lateral size was observed between the GO1 (unsonicated) and GO2 (sonicated) samples, of 29 µm and 9 µm respectively. This is because the GO1 (control) sample remained in its stacking manner, which eventually underwent exfoliation into GO nanosheets after sonication. Further increase in sonication time (GO2 - GO5) resulted in proportionate reduction of lateral size to 9 µm, 6µm, 4µm, and 2µm respectively as shown in Figure 2. These findings are supported by the study conducted by Lin et al. (2017) where significant reduction in lateral size was observed at the initial stage of sonication of graphene-based material. The changes in the lateral size of GOs are also in agreement with the observation made from Figure 1.

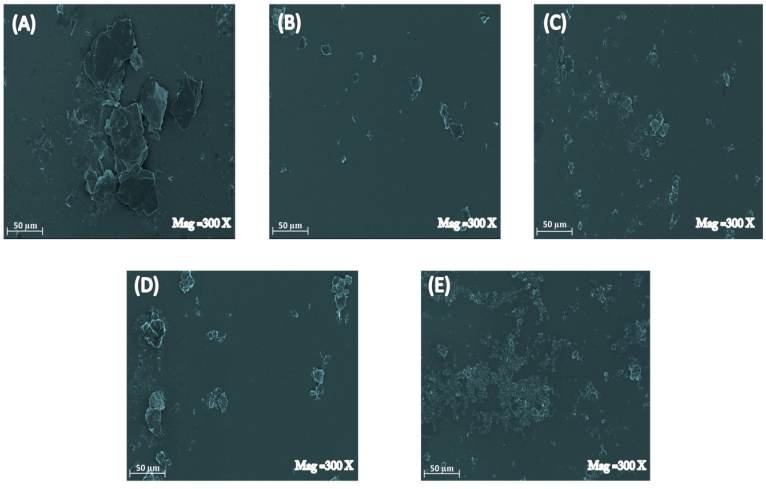

Figure 1. Micrographs of graphene oxide at different sonication times; (A) O minute (GO1); (B) 10 minutes (GO2); (C) 30 minutes (GO3); (D) 60 minutes (GO4); and (E) 100 minutes, at a magnification of 300X

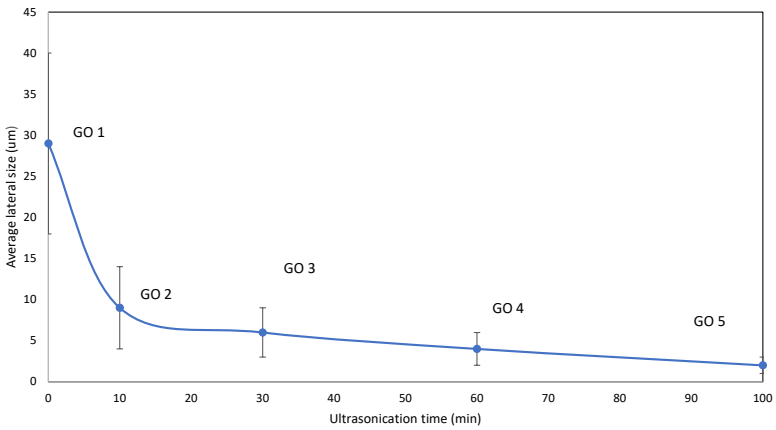

Figure 2. Average lateral sizes of control (GO1)/sonicated (GO2 - GO5) graphene oxide samples subjected to different ultrasonication times

Thermal Properties of PPD Composite Emulsion

Figure 3 displays the DSC heating cycle thermograms of the PPD emulsions with variable graphene oxide lateral sizes (GO1 - GO5). As can be seen, the addition of GO in the PPD emulsions generally lowered their melting point. Moreover, no clear pattern or trend was observed between the samples given the fluctuating thermal readings. However, the PPD emulsions thermal properties were found to remain unaffected (not exceeding EJN) with the addition of GO. EJGO5 displayed the lowest melting temperature, indicating that GO widens the temperature range of PPD emulsion by maintaining the fluidity of the emulsion. Upon heating, the emulsions, particularly EJN, EJGO2, and EJGO4, generated exothermic peaks of -63.51, -84.18, and -80.03°C respectively as presented in Table 2. This suggests that crystallisation had occurred before the melting point was reached. These peaks are referred as the devitrification peaks (Td). Devitrification or recrystallisation that occurs

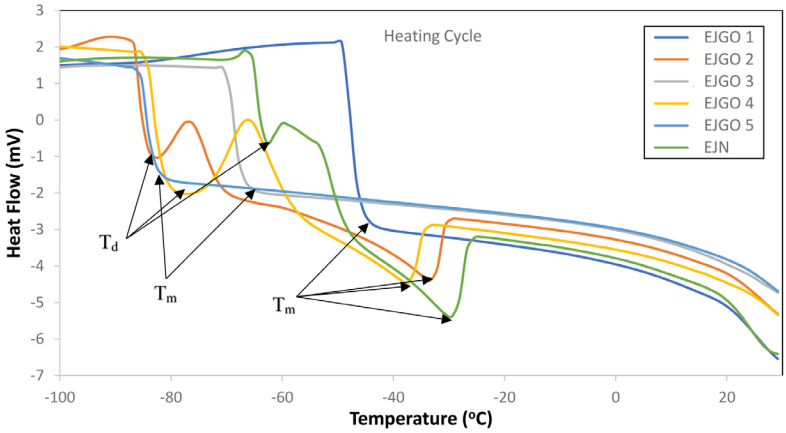

Figure 3. DSC heating cycle thermograms of PPD samples

during the reheating process of sample indicates no formation of ice crystals during its cooling process (Nasir et al., 2018). Accordingly, this phenomenon helps to eliminate the problem of neighbouring droplets collision due to volume expansion from the ice crystals formation. Therefore, the formation of large sized droplets could be avoided, and the stability of emulsions can be enhanced during the temperature cycle.

Pour Point Evaluation (ASTM D-97)

Figure 4 shows the pour point reduction (PPR) of the treated waxes with the EJN and EJGO1 - EJGO5 emulsions. The results indicated that the addition of graphene oxide, particularly in EJGO1 boosted the performance of the additive in reducing the pour point of the model oil to as minimum as 2^{o}C reduction compared to the control sample (EJN). The highest PPR of 10^{o}C was displayed by EJGO5 which has the smallest lateral size of 1 μm. This underlines the impact of lateral size manipulation in boosting the PPR of sonicated emulsions up to 100% compared to the unsonicated sample (EJGO1) which only yielded 5^{o}C PPR.

Theoretically, paraffin chains will adsorb and co-crystallise with polymers. This manifestation modifies the shape and size of the wax crystals. Furthermore, it encourages improvement in performance-wise as displayed by EJGO1 - EJGO5 in Figure 4 which is contributed by the presence of graphene oxide. This material provides secondary nucleation site for wax co-crystallisation. Besides, it also creates repulsive interaction among wax crystals (Al-Sabagh et al., 2016), which allows the wax crystals to remain dispersed without forming interlocking network, hence enhancing the flow-ability of model oil even at lower temperatures. Notably, smaller GO lateral size is achieved with longer ultrasonication duration, which provides more nucleation site for wax precipitation. Consequently, this reduces the tendency of wax particles crystallisation with one another by forming a rigid network that favours the flow improvement at a lower temperature.

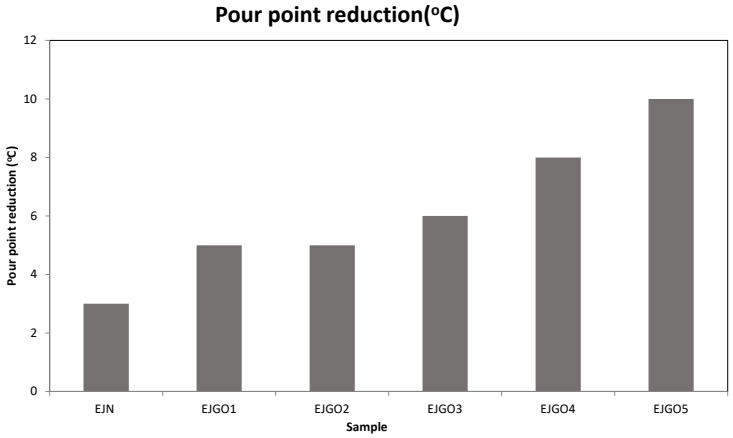

Figure 4. Pour point reduction of model oil injected with 1000 ppm PPD samples

Thermal Analysis of Model Oil

The DSC thermograms and wax crystallisation enthalpy of the wax samples are demonstrated in Figure 5 and Table 3 respectively. Generally, the addition of the control sample (EJN) was seen to increase the wax appearance temperature (WAT) value to about 4.71°C. This portrays the role of EVA as crystal nuclei to stimulate wax crystallisation at the initial stage before providing an inhibition effect.

On the other hand, EJGO5 demonstrated a WAT increment of 2.73°C, which was the lowest among all samples. This indicates that the addition of GO provides better efficiency in the modification of the wax crystallisation process. In addition, GO plays a major role in dispersing and stabilising wax crystals to inhibit aggregation so that high pour reduction can be achieved, as demonstrated in Figure 5. As such, GO provides heterogeneous nucleation sites for wax chains to co-crystallise, resulting in smaller wax aggregates and thus generating well-dispersed aggregates. Hence, the model oil remained in fluid state.

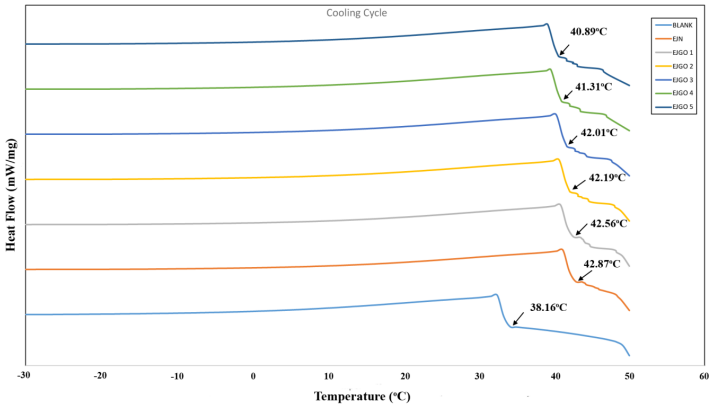

Figure 5. DSC thermograms of wax appearance temperature (WAT) of untreated/treated model oil

Based on Table 3, the samples with GO addition demonstrated lower wax crystal enthalpy values compared with the untreated and treated waxes with the reference sample (EJN). For instance, EJGO1 exhibited an enthalpy of 25.04 Jg^{-1}, lower than those of the untreated and treated EJN of 30.40 and 31.93 Jg^{-1} respectively. Further decrement in enthalpy was observed with the reduction in the lateral size of GO. Herein, the addition of GO decreased the ΔH_f and increased the critical radius (RC) (Yang et al., 2017), where EJGO5 exhibited the lowest enthalpy value of 23.97 Jg^{-1}. Enthalpy information can be used to evaluate the capability of a wax additive. Moreover, a lower enthalpy value indicates lesser amount of wax being precipitated or crystallised. Thus, better pour point inhibition can be achieved.

However, these findings are not aligned with the WAT results, as shown in Figure 5. This phenomenon plausibly arises due to the presence of GO particles which offers

heterogeneous nucleation sites for the aggregation of wax at smaller degrees of super cooling, therefore resulting in a minor escalation in the wax appearance temperature (WAT) readings.

Table 3

Wax crystallisation enthalpy of all samples

SAMPLE	ΔH_{wc} (Jg^{-1})
Untreated wax	30.40
EJN	31.93
EJGO 1	25.04
EJGO 2	25.06
EJGO 3	24.56
EJGO 4	24.34
EJGO 5	23.97

Polarised Optical Microscopy (POM)

The microstructures of the untreated/treated model oil observed at 20°C are as illustrated in Figure 6. As can be seen, the untreated model oil exhibited smaller wax crystal size compared to the treated EJN and EJGO1. A large amount of precipitated wax crystals was present in the untreated sample. The addition of EJN into the model oil had significantly altered the morphology of the wax crystals into larger wax precipitates, whereas the introduction of GO into the model oil resulted in smaller and more dispersed wax crystals as illustrated in Figure 6(C). GO particles are capable to improve the inhibition of wax growth via surface adsorption (Al-Sabagh et al., 2016), where they adsorb onto wax surfaces, causing the wax nuclei irresponsive towards temperature changes. This promotes the aggregation of wax; however in fine small size or in dispersed manner. Subsequently, the interlocking wax network, which is essential for solidification is eliminated.

The wax crystal microstructures of the model oil treated with EJGO1 - EJGO5 were observed and demonstrated in Figure 7. As shown in Figure 7(A), the wax crystals assembled as interlocking wax network. This occurrence shows that EJGO1 which has the highest lateral size of 29 µm exhibited the least efficiency in creating barrier to the formation of interlocking network. After the addition of EJGO2, the formation of wax network became lesser and more dispersed wax particles were observed. The reduced lateral size of GO favours further inhibition of interlocking network of wax crystals, as evident in Figure 7. Furthermore, even with the highest number of crystal aggregates, the wax aggregates in EJGO5 remained dispersed and stabilised given the adsorption of GO with the surplus nucleation site.

Apparently, more wax crystals were formed but in dispersed manner in EJGO5 than EJGO1, as observed by the very limited interlocking wax networks present in the model oil

as shown in Figure 7(E). Therefore, GO is deemed to impede the formation of interlocking crystal network, contributing to a lower pour point temperature. The deviations in wax morphology are in consent with the pour point results portrayed in Figure 4.

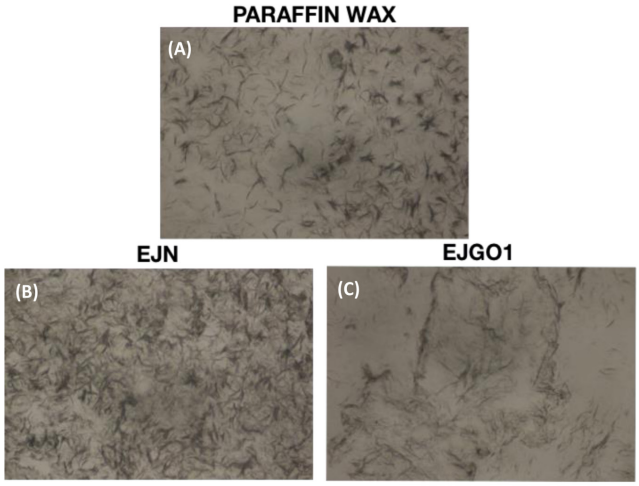

Figure 6. Polarised optical microscope images of the wax crystal microstructures of (A) untreated paraffin wax; (B) treated wax with EJN; and (C) treated wax with EJGO1

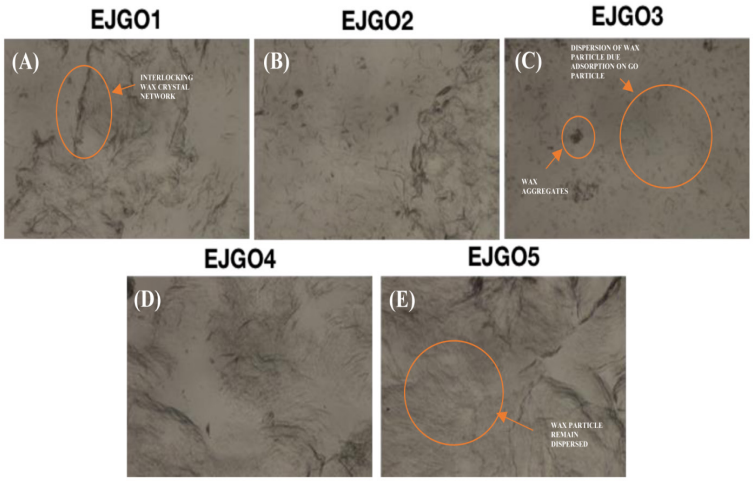

Figure 7. Polarised optical microscope images of wax crystal microstructures of treated waxes with (A) EJGO1; (B) EJGO2; (C) EJGO3; (D) EJGO4; and (E) EJGO5

CONCLUSION

The effects of variable GO lateral sizes on the pour point reduction (PPR) and wax crystallisation of model oil were investigated in this study. The properties of the PPD emulsions of study were also examined where no significant adverse effect was detected. However, contrasting influences of GO lateral size on the WAT and PPR parameters were

observed. It was also found that GO acts as the crystal nucleus to promote wax crystallisation, which eventually increased the WAT of emulsions. Nonetheless, EJGO5 reflected a higher PPR of 10^{o}C compared to the control sample (EJN) of only 3^{o}C. This finding is supported by the lowest wax crystallisation enthalpy of 23.97 Jg^{-1} displayed by EJGO5 which has the smallest GO lateral size. The study further verified that lateral size also played a significant role in altering wax crystallisation. Herein, smaller GO lateral size offers larger surface area for the adsorption of wax crystals, resulting in fewer wax aggregates formed with improved dispersion. Subsequently, improper wax crystals assembly gives rise to delayed formation of interlocking wax crystal network, which invariably reduces the pour point temperature. In conclusion, this study revealed the structure-activity relationship of GO lateral size effects on the thermal properties and microstructure of wax in model oil. The addition of GO in conventional PPD provides a positive boost towards wax crystallisation while retaining the original PPD emulsion thermal properties.

ACKNOWLEDGEMENTS

The authors are deeply indebted to Professor Azlan Ariffin and the laboratory team for their help and guidance throughout the completion of this research and publication. The authors would also like to express appreciation for the financial support awarded by the Ministry of Education Malaysia (MOE) via Fundamental Research Grant Scheme (FRGS) (Grant No. 203/PBAHAN/6071326).

REFERENCES

Admiral, A., Abdullah, M., & Ariffin, A. (2016). Evaluation of emulsified acrylate polymer and its pour point depressant performance. *Procedia Chemistry, 19*, 319-326.

Al-Sabagh, A., Betiha, M., Osman, D., Hashim, A., El-Sukkary, M., & Mahmoud, T. (2016). Preparation and evaluation of poly (methyl methacrylate)-graphene oxide nanohybrid polymers as pour point depressants and flow improvers for waxy crude oil. *Energy and Fuels, 30*(9), 7610-7621.

Boccaccini, A. R., Erol, M., Stark, W. J., Mohn, D., Hong, Z., & Mano, J. F. (2010). Polymer/bioactive glass nanocomposites for biomedical applications: A review. *Composites Science and Technology, 70*(13), 1764-1776.

Deshmukh, S., & Bharambe, D. (2008). Synthesis of polymeric pour point depressants for Nada crude oil (Gujarat, India) and its impact on oil rheology. *Fuel Processing Technology, 89*(3), 227-233.

Kim, J., Kim, S. W., Yun, H., & Kim, B. J. (2017). Impact of size control of graphene oxide nanosheets for enhancing electrical and mechanical properties of carbon nanotube–polymer composites. *RSC Advances, 7*(48), 30221-30228.

Li, H., Wu, X., Cheng, K., Miao, J., Tang, Z., Qiu, H., & Yang, J. (2019). Preparation of graphene oxide with large lateral size and graphene/polyimide hybrid film via in situ “molecular welding” strategy. *Materials Letters, 237*, 168-171.

Lin, Z., Karthik, P., Hada, M., Nishikawa, T., & Hayashi, Y. (2017). Simple technique of exfoliation and dispersion of multilayer graphene from natural graphite by ozone-assisted sonication. *Nanomaterials, 7*(6), 1-10.

Martínez-Palou, R., de Lourdes Mosqueira, M., Zapata-Rendón, B., Mar-Juárez, E., Bernal-Huicochea, C., de la Cruz Clavel-López, J., & Aburto, J. (2011). Transportation of heavy and extra-heavy crude oil by pipeline: A review. *Journal of Petroleum Science and Engineering, 75*(3), 274-282.

Nasir, N., Rosdi, M., & Ariffin, A. (2018). The impact of different antifreeze agents on the thermal properties of ethylene vinyl acetate emulsion. *Polymers for Advanced Technologies, 29*(2), 708-715.

Pedersen, K. S., & Rønningsen, H. P. (2003). Influence of wax inhibitors on wax appearance temperature, pour point, and viscosity of waxy crude oils. *Energy and Fuels, 17*(2), 321-328.

Razak, A. S. A., Gafri, N. F., Razali, M. A. A., Ariff, Z. M., Hamid, Z. A. A., & Ariffin, A. (2018). The impact of monomer loading on poly (methyl methacrylate) nano emulsion as pour point depressant. *Petroleum Science and Technology, 36*(11), 793-800.

Rosdi, M., Ariffin, A., & Ishak, Z. (2016). Optimizing homogenization parameters for improving ethylene vinyl acetate emulsion stability in pour point depressant application. *Journal of King Saud University-Engineering Sciences, 30*(2), 105-115.

Sharma, R., Mahto, V., & Vuthaluru, H. (2019). Synthesis of PMMA/modified graphene oxide nanocomposite pour point depressant and its effect on the flow properties of Indian waxy crude oil. *Fuel, 235*, 1245-1259.

Umoruddin, N., Rosdi, M. H., & Ariffin, A. (2019). Mixed surfactant enabled EVA emulsion for PPD applications. *Journal of Dispersion Science and Technology, 40*(3), 361-368.

Yang, F., Yao, B., Li, C., Shi, X., Sun, G., & Ma, X. (2017). Performance improvement of the ethylene-vinyl acetate copolymer (EVA) pour point depressant by small dosages of the polymethylsilsesquioxane (PMSQ) microsphere: An experimental study. *Fuel, 207*, 204-213.

Yang, F., Zhao, Y., Sjöblom, J., Li, C., & Paso, K. G. (2015). Polymeric wax inhibitors and pour point depressants for waxy crude oils: A critical review. *Journal of Dispersion Science and Technology, 36*(2), 213-225.

Zhao, Z., Yan, S., Lian, J., Chang, W., Xue, Y., He, Z., ... & Han, S. (2018). A new kind of nanohybrid poly (tetradecyl methyl-acrylate)-graphene oxide as pour point depressant to evaluate the cold flow properties and exhaust gas emissions of diesel fuels. *Fuel, 216*, 818-825.